HOSTED BY

ELSEVIER

Available online at www.sciencedirect.com

ScienceDirect

Journal of Magnesium and Alloys 3 (2015) 180–187
www.elsevier.com/journals/journal-of-magnesium-and-alloys/2213-9567

Full Length Article

Microstructural evolution of Mg-7Al-2Sn Mg alloy during multi-directional impact forging

M.G. Jiang [a,b], H. Yan [a,*], L. Gao [c,**], R.S. Chen [a]

[a] *The Group of Magnesium Alloys and Their Applications, Institute of Metal Research, Chinese Academy of Sciences, 62 Wencui Road, Shenyang 110016, China*
[b] *University of Chinese Academy of Sciences, 19 Yuquan Road, Beijing 100049, China*
[c] *General Motors China Science Lab, 56 Jinwan Road, Pudong, Shanghai 201206, China*

Received 22 September 2014; revised 17 August 2015; accepted 25 August 2015

Available online 1 October 2015

Abstract

Multi-directional impact forging (MDIF) was applied to a Mg-7Al-2Sn (wt.%) Mg alloy to investigate its effect on the microstructural evolution. MDIF process exhibited high grain refinement efficiency. After MDIF 200 passes, the grain size drastically decreased to 20 μm from the initial coarse grains of ~500 μm due to dynamic recrystallization (DRX). Meanwhile, original grain boundaries remained during MDIF and large numbers of fine spherical β-$Mg_{17}Al_{12}$ particles dynamically precipitated along the original grain boundaries with high Al concentration, acting as effective pinning obstacles for the suppression of DRXed grain growth. Besides, micro-cracks nucleated during MDIF and propagated along the interface between the remained globular or cubic Al-Mn particles and Mg matrix.

Keywords: Magnesium alloy; Forging; Grain refinement; Dynamic precipitation

1. Introduction

Magnesium (Mg) alloys are becoming increasingly attractive for potential application in the automobiles and aerospace industries because of low density and high specific strength. However, due to the hexagonal close-packed (HCP) structures, Mg alloys usually exhibit undesirable ductility and strength at ambient conditions, which limits their widespread application.

Grain refinement has proven to be an effective approach to overcome the current drawbacks of Mg alloys. Therefore, various methods have been applied to Mg alloys to improve the mechanical properties by grain refinement, such as equal channel angular extrusion (ECAE) [1,2], cyclic extrusion and compression (CEC) [3,4], friction stir processing (FSP) [5,6] and multi-directional forging (MDF) [7,8]. Feng et al. [5] reported that FSP resulted in remarkable grain refinement (from coarse as-cast grains to ~15 μm) in an as-cast AZ91 Mg alloy, thereby improving significantly the mechanical properties. Miura et al. [7] applied MDF to an AZ61 Mg alloy and obtained ultrafine grains of ~0.6 μm, and consequently, an excellent balance of strength and ductility (yield stress of 480 MPa and elongation 5%). However, these methods still stay at laboratory-scale research at the present due to small size of processed sample, complicated processing procedure and expensive equipment, which directly leads to low production efficiency and high production costs. In our previous study [9], multi-directional impact forging (MDIF) was newly proposed and successfully applied to an AZ61 Mg alloy. MDIF exhibited high grain refinement efficiency, and has proven to be a simple and highly efficient method to synchronously enhance strength and ductility.

On the other hand, Mg-Al-Sn (AT) Mg alloy [10] was newly designed by General Motors for automotive structural applications and exhibited more balanced mechanical properties and higher thermal stability compared to AZ91 alloy. In this study, therefore, this Mg-7Al-2Sn (wt.%) alloy was subjected to MDIF and the microstructural evolution during MDIF process was investigated in detail.

* Corresponding author. The Group of Magnesium Alloys and Their Applications, Institute of Metal Research, Chinese Academy of Sciences, 62 Wencui Road, Shenyang 110016, China. Tel.: +86 24 23926646; fax: +86 24 23894149.
E-mail address: hyan@imr.ac.cn (H. Yan).
** Corresponding author. General Motors China Science Lab, 56 Jinwan Road, Pudong, Shanghai 201206, China. Tel.: +86 21 28987160; fax: +86 21 58321165.
E-mail address: lei.gao@gm.com (L. Gao).

http://dx.doi.org/10.1016/j.jma.2015.08.005
2213-9567/

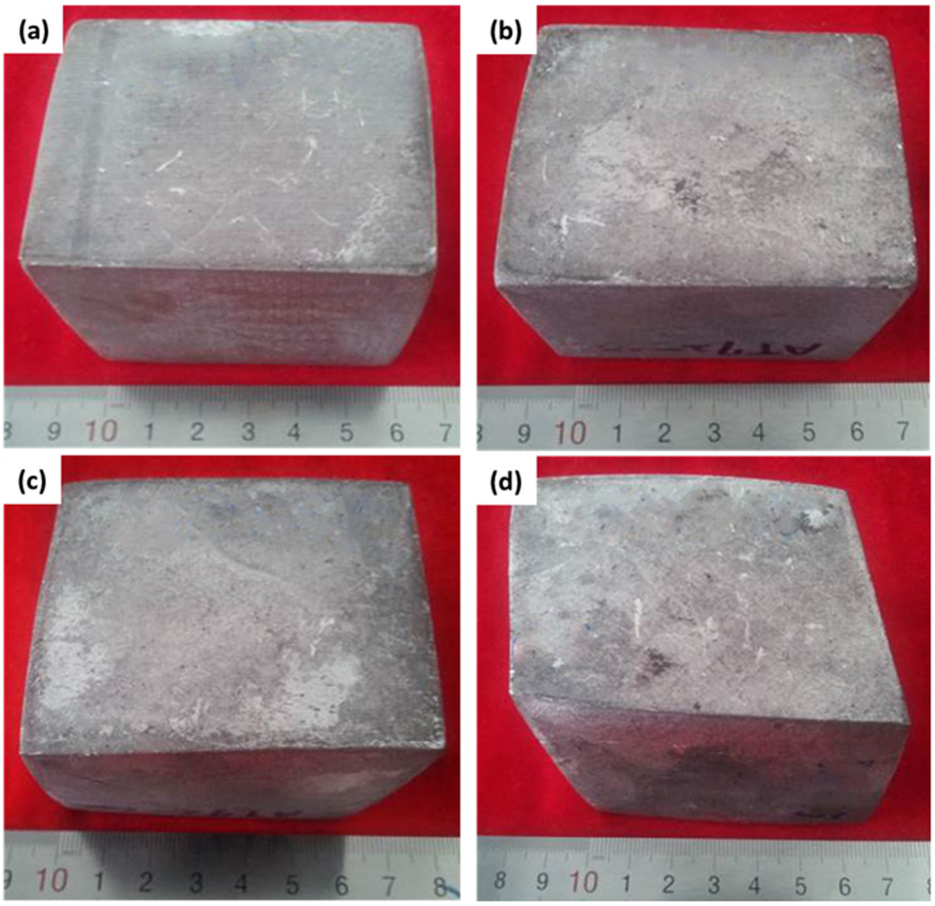

Fig. 1. Macroscopic morphology of cubic AT72 alloy samples after MDIF (a) 20, (b) 50, (c) 100 and (d) 200 passes.

2. Experimental procedures

The material used in this study was AT72 Mg alloy (6.88 wt.% Al, 1.94 wt.% Sn, 0.33 wt.% Mn, and -balance Mg). Cubic block samples with a dimension of 65 mm × 65 mm × 65 mm were machined from as-cast AT72 Mg ingot and solution treated at 420 °C for 24 h. Prior to MDIF process, these samples were heated to the processing temperature of 300 °C in an electric resistant furnace and kept for 30 min. MDIF process was carried out using an industrial air pneumatic hammer machine according to the procedures described in our previous study [9]. In brief, the forging direction was changed by 90° from pass to pass (i.e. X to Y to Z to X to…). The cubic samples were MDIFed to different forging passes and finally cooled down in air. All the MDIFed samples were free from any surface defects as shown in Fig. 1.

Microstructure was observed on the central part of the cubic samples parallel to the last forging direction (LFD), as shown in Fig. 2, using optical microscopy (OM) and scanning electron microscopy (SEM, Philips XL30 ESEM-FEG/EDAX) equipped with an attached energy-dispersive X-ray (EDX). The specimens for the microstructural observation were etched with acetic picral (2 g of picric acid, 5 ml of acetic acid, 5 ml of water and 25 ml of ethanol).

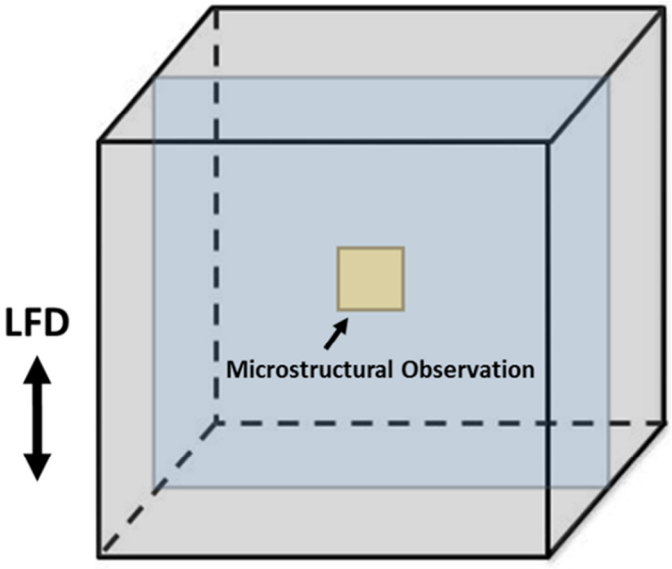

Fig. 2. Schematic illustration of microstructural observation spot in the MDIFed cubic samples. LFD refers to last forging direction.

3. Results and discussion

3.1. Microstructures before MDIF process

Fig. 3 shows the microstructures of as-cast AT72 alloy and corresponding EDX results of the second phase particles. The as-cast alloy (Fig. 3a) exhibited a typical network eutectic microstructure comprising of α-Mg matrix and coarse eutectic intermetallic phases distributing along the grain boundaries and within the grain interiors. The BSE image (Fig. 3b) shows that the coarse eutectic phases distributing at the grain boundaries consisted of second phases A and B. The corresponding EDX results of these second phases reveal that second phases A and B were β-$Mg_{17}Al_{12}$ and Mg_2Sn, respectively, which is consistent with the results reported by Luo et al. [10]. According to the binary phase diagram [11], the binary eutectic temperatures of $Mg_{17}Al_{12}$ and Mg_2Sn phases are 437 °C and 562 °C, respectively. Higher thermal stability of Mg_2Sn phase makes it more difficult to be dissolved through solution treatment.

Fig. 4a shows the optical microstructure of AT72 alloy after solution treatment at 420 °C for 24 h. The grains were dramatically coarsened up to ~500 μm and network eutectic phases were remarkably dissolved into the Mg matrix, thereby resulting in a supersaturated solid solution. However, it can be seen that some globular or cubic second phase particles still existed within the grain interiors. According to the EDX result in Fig. 4b, these remained particles within grain interiors were determined to be Al-Mn second phase rather than Mg_2Sn considering the negligible Sn concentration. Different from our expectation, no Mg_2Sn phase was detected by EDX analysis. Thus, it can be deduced that Mg_2Sn phase was dissolved into the Mg matrix during solution treatment. In Mg-Al alloys, Al-Mn particles are usually observed in the micrograph as globular morphology, which could be Al_4Mn [12,13] or Al_8Mn_5 [14,15]. These globular or cubic Al-Mn phase particles remained during solution treatment play an important role in the MDIF process, which will be discussed later in detail.

3.2. Microstructures after MDIF process

Fig. 5 shows the microstructures of MDIFed AT72 alloy with different forging passes. Obviously, the initial coarse grains of ~500 μm were significantly refined due to dynamic

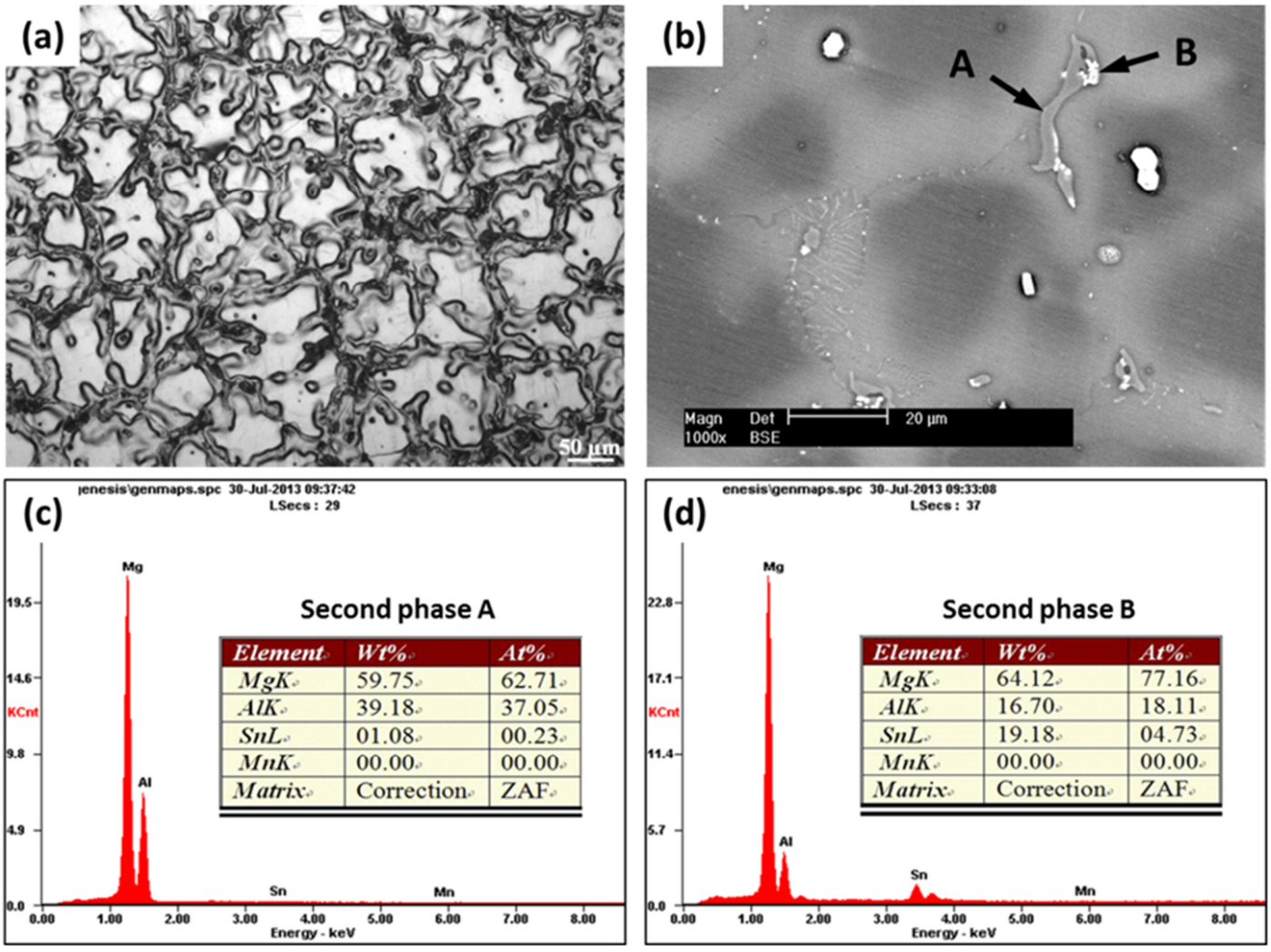

Fig. 3. (a) Optical, (b) BSE images of as-cast AT72 alloy and (c, d) corresponding EDX results of the second phase particles indicated in the image (b).

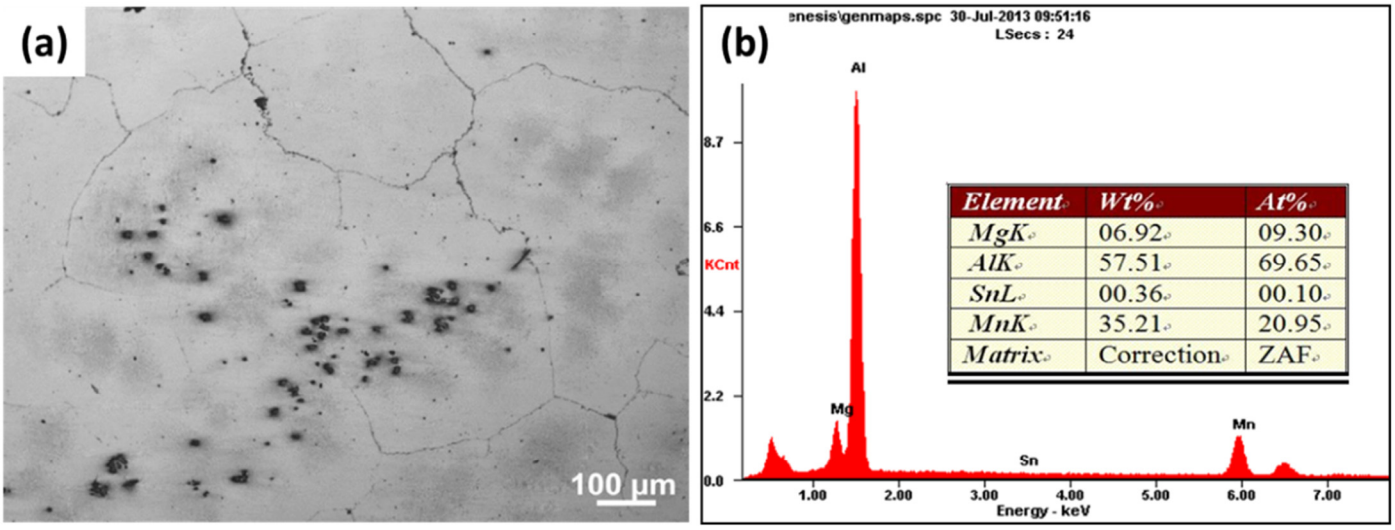

Fig. 4. (a) Optical microstructure of solution treated AT72 alloy and (b) EDX result of the remained particles within grain interiors after solution treatment.

recrystallization (DRX), suggesting the high grain refinement efficiency of MDIF process.

After 20 forging passes, as shown in Fig. 5a and b, grain structure was inhomogeneous and consisted of relatively coarse DRXed grains of ~60 μm in the regions indicated by the blue circles and fine DRXed grains of ~20 μm in the regions indicated by the white circles. Jin et al. [16] reported that the uneven rate of DRX at different grains was responsible for the inhomogeneous microstructures. Apparently, the regions containing the coarse and fine grains were separately distributed in different original grains, as indicated by blue and white circles in Fig. 5a, which means that these different original grains experienced uneven rate of DRX. Thus, the inhomogeneous grain structure in this work was related to the uneven recrystallization rate due to the different orientations of original grains. Furthermore, our previous study [17] revealed the grain refinement evolution during MDIF in an AZ61 Mg alloy and proposed that the uneven rate of DRX in the early forging passes was ascribed to the activation of different twin types in different original grains. However, the microstructures during initial MDIF process were not studied in this study.

With increasing forging passes to 50 passes, the relatively coarse DRXed grains in some original grains shown in Fig. 5a are consumed by further DRX process (Fig. 5c and d). After forging 100 passes, homogenous grain structure in different original grains was achieved and the average grain size of DRXed grains was ~35 μm (Fig. 5e and f). With continuous forging up to 200 passes, homogenous equiaxial DRXed grains of ~20 μm were achieved (Fig. 5g and h), indicating that DRX in different original grains had been nearly completed. This further grain refinement by DRX can be ascribed to continuous change of forging direction from pass to pass during MDIF. The orientation relationship between basal planes of grains and loading direction is always changing unlike rolling process [16], i.e., the basal plane of some grains is perpendicular to the compression stress, which is not favorable for basal slip due to the nearly zero resolved shear stress. Thus, the dominant basal slip in the relatively coarse grains always stays active during MDIF. Besides, even non-basal slips are likely to operate due to grain refinement and high temperature stimulation (~300 °C). Sitdikov et al. [18] reported that the interaction between basal slip dislocations and non-basal slip dislocations facilitates the formation of sub-grain boundaries and such sub-grain boundaries gradually lead to the development of high angle grain boundaries with increasing strain, finally forming new DRXed grains. Meanwhile combined with the results in our previous study [17], it can be determined that discontinuous DRX mechanism is responsible for the further grain refinement of the relatively coarse DRXed grains after 20 forging passes, finally resulting in a homogenous microstructure with grains of ~20 μm.

Besides the grain refinement, another two aspects, i.e., the original grain boundaries and dynamic precipitation need to be mentioned. Original grain boundaries indicated by white arrows in Fig. 5 were easily observed and no tendency of disappearance was detected during the whole MDIF process. Dynamic precipitation in dark color was formed along original grain boundaries as shown in Fig. 5. It can be clearly seen in the magnified images in Fig. 6 that fine spherical second phase particles less than 1 μm dynamically precipitated near the original grain boundaries. EDX result (Fig. 6d) reveals that these globular second phase particles were β-$Mg_{17}Al_{12}$ rather than Mg_2Sn. For Mg-Al alloys, it takes up to about 40 h to achieve the complete dissolution of the eutectic β-phase due to low diffusion rate of Al in Mg [19]. In this case, solution treatment at 420 °C for 24 h could not provide sufficient time for uniform distribution of solute Al atoms into the Mg matrix, resulting in the higher Al concentration near original grain boundaries than within grain interiors. Thus, when samples were subjected to MDIF, β-$Mg_{17}Al_{12}$ phase particles were preferentially formed along original grain boundaries with higher Al concentration regions and spherical shaped particles dynamically precipitated from the energy perspective. Much finer DRXed grains of less than 3 μm were observed in Fig. 6c, which indicates that homogenously distributed β-$Mg_{17}Al_{12}$ precipitates near original

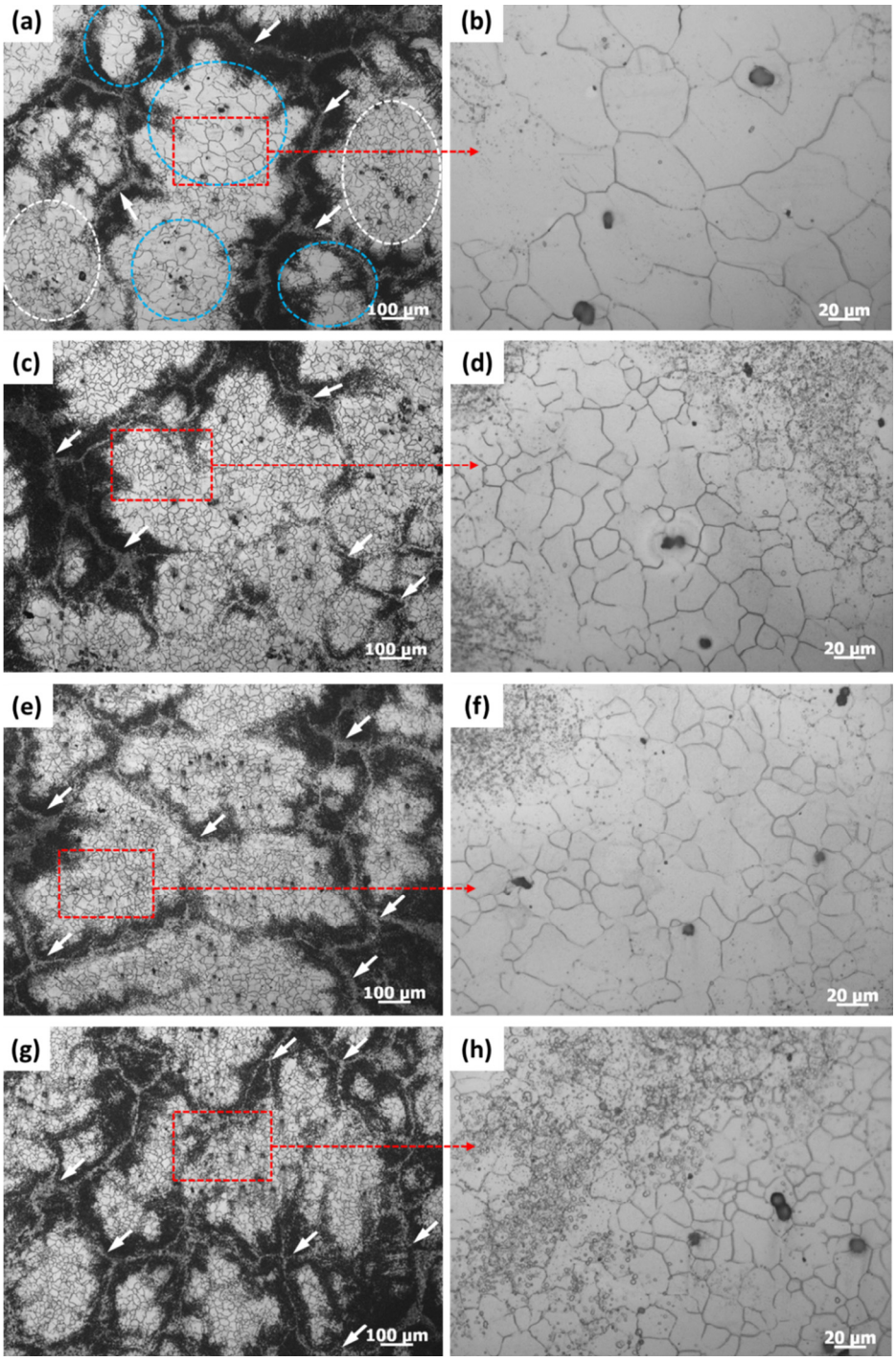

Fig. 5. Optical microstructures of AT72 alloy samples after MDIF (a, b) 20, (c, d) 50, (e, f) 100 and (g, h) 200 passes. Blue and white circles in (a) indicate the region of coarse and fine grains, respectively. White arrows indicate the original grain boundaries.

grain boundaries were effective pinning obstacles for suppressing the DRXed grain growth.

Fig. 7 shows the SEM images of micro-cracks and EDX results of the globular or cubic particles in AT72 alloy samples forged to different passes. Apparently, micro-cracks propagated along the globular or cubic particles irrespective of forging passes. EDX results in Fig. 7 reveal that these particles were Al-Mn phase, which could be Al_4Mn [12,13] or Al_8Mn_5 [14,15]. The corresponding average Al/Mn weight ratio in these particles was around 1.61, which is close to the ratio of 1.96 for Al_4Mn. According to the Al-Mn equilibrium phase diagram [11], the concentration of Mn (0.33 wt.%) in AT72 alloy is sufficient to form Al-Mn particles. The melting point of Al-Mn phase is as high as 658 °C, which is much higher than that of β-$Mg_{17}Al_{12}$ (437 °C) and Mg_2Sn phase (562 °C). Thus, these globular or cubic Al-Mn particles remained stable during

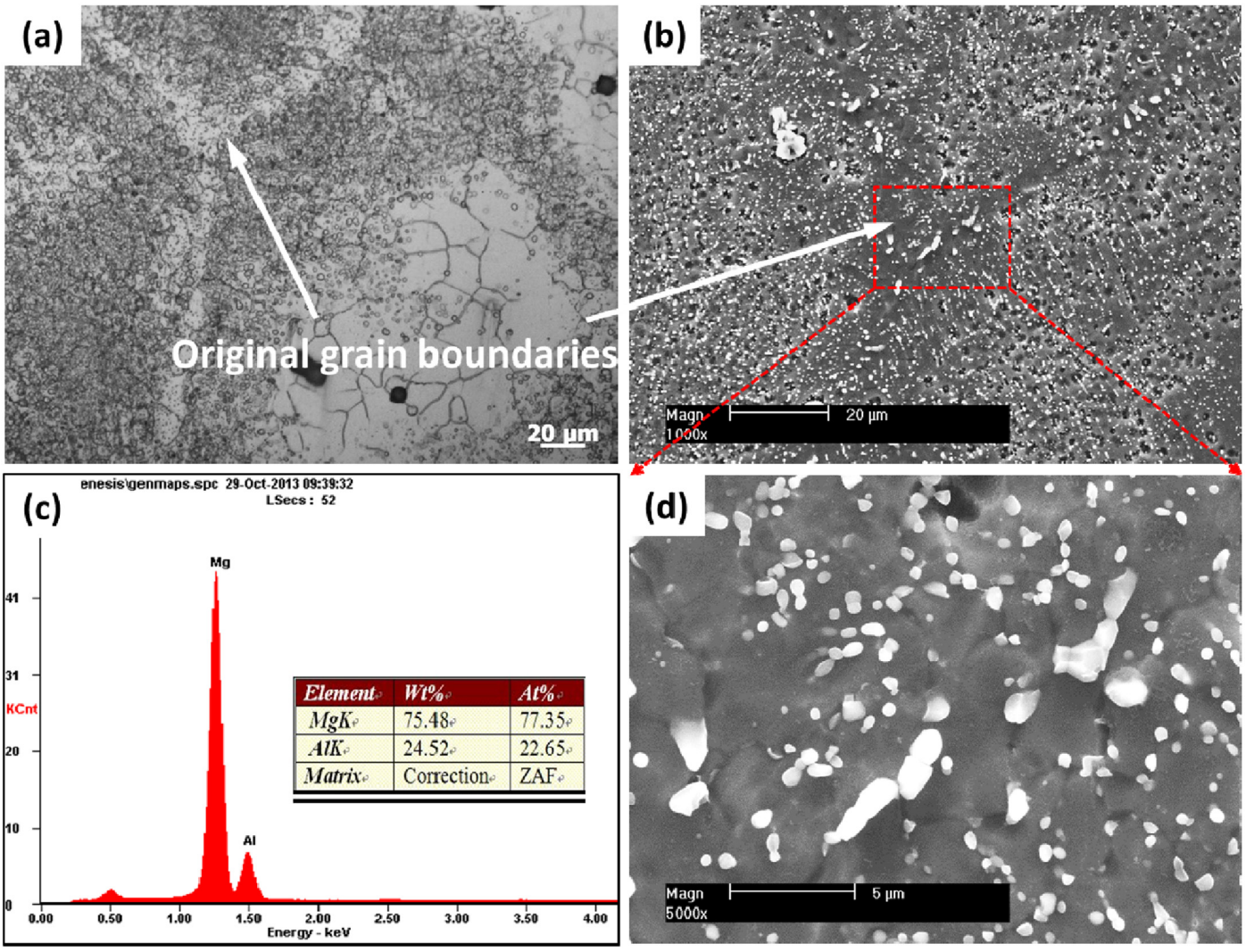

Fig. 6. (a) Optical, (b, d) SEM images and (c) corresponding EDX result of dynamic precipitation in AT72 alloy sample after MDIF 200 passes.

solution treatment due to their higher thermal stability. It can be clearly observed that micro-cracks propagated along the Al-Mn particles aggregated area, which may be related to the progressively accumulated stress during MDIF process. Micro-cracks would be initiated at the interface between the globular or cubic particles and the matrix. With further deformation, micro-cracks propagated along these particles to release the accumulated stress. The relationship between the micro-cracks and second phase during deformation has been discussed in many studies [5,14,20]. Chen et al. [14] reported that micro-cracks nucleated at the interface between the β-$Mg_{17}Al_{12}$ phase and the matrix during tensile deformation, which is ascribed to incompatibility between the body-centered cubic structure of β-$Mg_{17}Al_{12}$ phase and HCP structure of Mg matrix. In this work, micro-cracks were possible due to incompatibility between Al-Mn phase and the Mg matrix.

4. Conclusions

In this study, MDIF process was applied to AT72 Mg alloy and the microstructural evolution was investigated. After MDIF 20 passes, inhomogeneous grain structure formed due to uneven rate of DRX in different original grains. With continuous forging up to 200 passes, fully DRXed microstructure was obtained with fine grains of 20 μm, suggesting the high grain refinement efficiency of MDIF process. Meanwhile, large numbers of fine spherical shaped β-$Mg_{17}Al_{12}$ phase dynamically precipitated along the original grain boundaries with high Al concentration during MDIF, acting as effective pinning obstacles for the suppression of DRXed grain growth. Besides, micro-cracks nucleated during MDIF and propagated along the interface between the remained globular or cubic Al-Mn particles and Mg matrix.

Acknowledgements

The authors gratefully acknowledge the financial support from General Motors Corporation, the National Basic Research Program of China (973 Program, No. 2013CB632202) and National Natural Science Foundation of China (NSFC, No. 51301173).

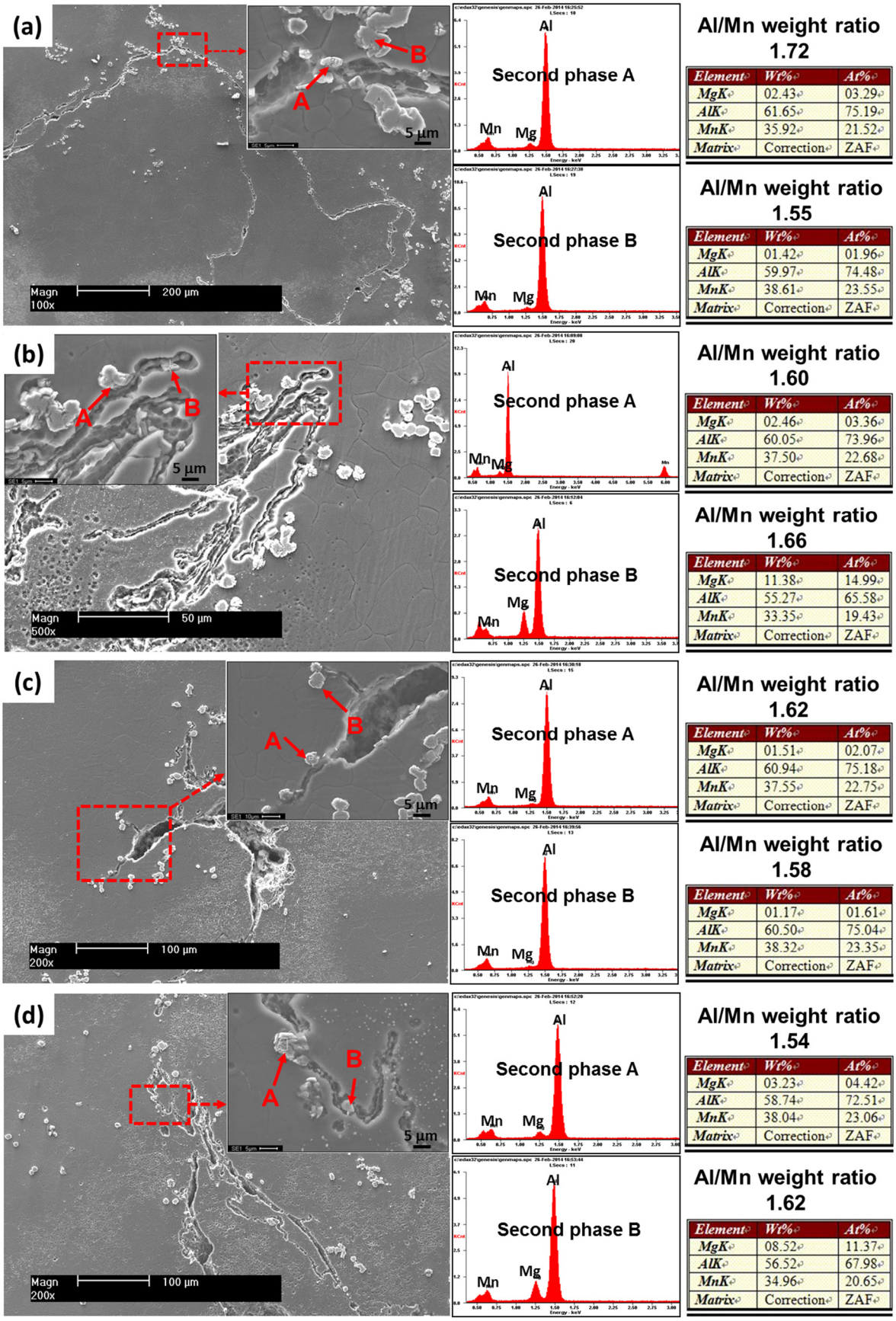

Fig. 7. SEM images of micro-cracks and EDX results of the globular or cubic particles in AT72 alloy samples after MDIF (a) 20, (b) 50, (c) 100 and (d) 200 passes.

References

[1] S. Ding, W. Lee, C. Chang, L. Chang, P. Kao, SCR Mater 59 (2008) 1006–1009.
[2] W. Tang, R. Chen, J. Zhou, E. Han, Mater. Sci. Eng. A 499 (2009) 404–410.
[3] J. Lin, Q. Wang, L. Peng, H.J. Roven, J. Alloys Comp. 476 (2009) 441–445.
[4] W. Zhang, Y. Yu, X. Zhang, W. Chen, E. Wang, Mater. Sci. Eng. A 600 (2014) 181–187.
[5] A. Feng, Z. Ma, SCR Mater 56 (2007) 397–400.
[6] W. Yuan, R. Mishra, Mater. Sci. Eng. A 558 (2012) 716–724.
[7] H. Miura, T. Maruoka, X. Yang, J.J. Jonas, SCR Mater 66 (2012) 49–51.
[8] W. Yuan-Zhi, Y. Hong-Ge, C. Ji-Hua, D. Yong-Guo, Z. Su-Qin, S. Bin, Mater. Sci. Eng. A 556 (2012) 164–169.
[9] M.G. Jiang, H. Yan, R.S. Chen, Mater. Sci. Eng. A 621 (2015) 204–211.
[10] A.A. Luo, P. Fu, L. Peng, X. Kang, Z. Li, T. Zhu, Metall. Mater. Trans. A 43 (2012) 360–368.
[11] A.A. Nayeb-Hashemi, J.B. Clark, Phase Diagram of Binary Magnesium Alloys, ASM International, Materials Parks, OH, 1988.
[12] I.A. Yakubtsov, B.J. Diak, C.A. Sager, B. Bhattacharya, W.D. MacDonald, M. Niewczas, Mater. Sci. Eng. A 496 (2008) 247–255.
[13] H. Asgari, J.A. Szpunar, A.G. Odeshi, Mater. Des. 61 (2014) 26–34.
[14] B. Chen, D.-L. Lin, L. Jin, X.-Q. Zeng, C. Lu, Mater. Sci. Eng. A 483–84 (2008) 113–116.
[15] Y. Wang, M. Xia, Z. Fan, X. Zhou, G.E. Thompson, Intermetallics 18 (2010) 1683–1689.
[16] Q. Jin, S.-Y. Shim, S.-G. Lim, SCR Mater 55 (2006) 843–846.
[17] M.G. Jiang, H. Yan, R.S. Chen, J. Alloys Comp. 650 (2015) 399–409.
[18] O. Sitdikov, R. Kaibyshev, Mater. Trans. 42 (2001) 1928–1937.
[19] S. Kleiner, O. Beffort, P. Uggowitzer, SCR Mater 51 (2004) 405–410.
[20] H. Yan, S. Xu, R. Chen, S. Kamado, T. Honma, E. Han, J. Alloys Comp. 566 (2013) 98–107.